ELSEVIER

International Journal of Mass Spectrometry 195/196 (2000) 411–418

International Journal of Mass Spectrometry

Temperature and pressure effects on the elimination reactions of diethyl ether with hydroxide and amide ions

Michael C. Baschky, Steven R. Kass*

Department of Chemistry, University of Minnesota, Minneapolis, MN 55455, USA

Received 7 June 1999; accepted 7 September 1999

Abstract

Hydroxide and amide ion-induced elimination reactions of diethyl ether and diethyl ether-d_{10} were investigated with a variable temperature flowing afterglow apparatus. Temperature effects on reaction rates, kinetic isotope effects, and product distributions are reported. The pressure dependence of these transformations also were explored and mechanistic arguments are presented. This data confirms predictions based on statistical rate theory and *ab initio* calculations and provides valuable information on the potential energy surfaces for base-induced eliminations. (Int J Mass Spectrom 195/196 (2000) 411–418)

Keywords: Eliminations; Isotope effects; Kinetics; Diethyl ether; Flowing afterglow

1. Introduction

Elimination reactions are one of the most fundamental transformations in organic chemistry and have been extensively studied in solution ever since the time of Ingold and Hughes, who first proposed a nomenclature system to deal with these processes (i.e. E1, E2, and E1cb) [1,2]. Numerous mechanistic investigations have been carried out and a great wealth of information has been amassed. A detailed understanding of these processes, however, is hindered by the effect solvation, ion-pairing, and aggregation can have on reaction rates, intermediates, and selectivity. The intrinsic reactivity, consequently, is of special interest. This makes gas-phase data and ab initio molecular orbital calculations particularly valuable.

In the gas phase it is inherently difficult to differentiate between anion-induced elimination reactions and nucleophilic substitutions because both pathways can lead to the same ionic products. Nevertheless, elimination reactions have been extensively investigated and subtle questions dealing with regio- and stereochemical preferences have been probed by carrying out carefully designed product (ions and neutrals), kinetic, labeling, and isotope effect studies [3–17]. One of the most extensively examined processes involves the reaction of diethyl ether with hydroxide or amide ion [3–5,18–22].

$$Et_2O + B^- \rightarrow EtO^-{\cdot}BH + C_2H_4 \qquad (1a)$$

$$\Delta H^\circ_{rxn} = -18.2 \text{ kcal mol}^{-1} (B^- = HO^-)$$

* Corresponding author.

In memory of Professor Robert R. Squires, an outstanding scientist and a friend to many.

1387-3806/00/$20.00
PII S1387-3806(99)00196-7

$$\rightarrow EtO^- + BH + C_2H_4 \quad (1b)$$

$$\Delta H^\circ_{rxn} = +5.5 \text{ kcal mol}^{-1} (B^- = HO^-)$$

$$= -8.9 \text{ kcal mol}^{-1} (B^- = H_2N^-)$$

$$\rightarrow EtO^- + EtB \quad (1c)$$

$$\Delta H^\circ_{rxn} = -5.4 \text{ kcal mol}^{-} (B^- = HO^-)$$

$$= -21.8 \text{ kcal mol}^{-} (B^- = H_2N^-)$$

The resulting cluster ion ($EtO^-{\cdot}H_2O$ or $EtO^-{\cdot}H_3N$) must be formed from an elimination reaction [23], whereas the free ethoxide is mechanistically more ambiguous. It has been convincingly argued that EtO^- arises solely from an elimination reaction, as opposed to the thermodynamically more favorable substitution pathway, based upon the following. (1) Dimethyl ether does not react with HO^- or H_2N^- despite the fact that it is less hindered than diethyl ether. (2) Strain free cyclic ethers such as tetrahydrofuran and tetrahydropyran react via elimination reactions rather than nucleophilic substitutions. The two pathways can be distinguished in these cases simply by the mass-to-charge ratio of the product ions. (3) $^{18}OH^-$ reacts with diethyl ether to afford EtO^- and $EtO^-{\cdot}H_2{}^{18}O$ but not any $Et^{18}O^-$ as expected from the competing substitution pathway. (4) Large primary kinetic isotope effects have been observed. (5) Ab initio calculations predict lower barriers for eliminations than nucleophilic substitutions in analogous systems [24–32]. Statistical rate theory also has been used to model the reactions of Et_2O with HO^- and H_2N^- and a negative temperature dependence has been predicted for these reactions [3].

In this article we report on the temperature and pressure dependence of the reaction between diethyl ether and hydroxide or amide ion. Rate constants, kinetic isotope effects, and branching ratios have been measured, in part, to test Bierbaum et al. [3] and de Koning and Nibbering's [5] proposals that these reactions should display negative temperature dependences. In addition, this system provides a platform for examining a primary kinetic isotope effect as a function of temperature. It is well known that isotope effects are enormously valuable mechanistically in the liquid phase and that they increase exponentially (or faster) with decreasing temperature whereas the analogous behavior in the gas phase has not been extensively explored.

2. Experimental

A variable temperature flowing afterglow (FA) device, which has previously been described, was used for these experiments [33,34]. Amide and hydroxide ions were generated by electron ionization of ammonia and a 2:1 methane–nitrous oxide mixture, respectively. These ions and the helium buffer gas ($P_{He} \approx 0.35$ Torr and $\bar{v}_{He} \approx 8000$ cm s^{-1}) were allowed to flow 31–51 cm before coming into contact with diethyl ether so as to insure that laminar flow and temperature equilibration were established before the reaction of interest was initiated. Diethyl ether was added into the instrument by admitting the vapor above a liquid sample through a "shower head" type inlet which faces upstream, has 24 evenly spaced holes, and is symmetrically oriented around the center of the flow tube. The ions passed through a narrow orifice (nose cone), and were focused with a series of lens elements and mass selected either with a quadrupole or triple quadrupole mass filter before being detected using standard pulsing counting techniques.

Second-order rate constants were measured under pseudo-first-order conditions by adding varying amounts of diethyl ether via a Tylan Co. calibrated flow meter or flow controller. In order to accurately control the flow of the ether, the liquid sample was maintained at 0 °C by using an ice bath. Rate constants were obtained in a standard way by application of the following equation:

$$k = (-d \ln[A^-]/dF_B)[(F_{He})^2T^2/(P_{He})^2z] \ 1.10 \times 10^{-20} \quad (2)$$

where A^- is the reactant ion (HO^- or H_2N^-) signal intensity, F_B is the diethyl ether flow rate in STP cm^3 s^{-1}, F_{He} is the helium buffer gas flow rate in STP cm^3 s^{-1}, T is the temperature in kelvin, P_{He} is the flow tube pressure in Torr, z is the reaction distance in

Table 1
Rate constants for the reactions of hydroxide and amide ions with diethyl ether and diethyl ether-d_{10} at different temperatures[a]

T (°C)	B^-	k_H	Efficiency[b]	k_D	Efficiency[b]	k_H/k_D[c]
200	HO^-	2.8 ± 0.2	0.13 (0.12)	1.2 ± 0.2	0.056 (0.054)	2.3 ± 0.4
100	HO^-	3.8 ± 0.4	0.17 (0.16)	1.6 ± 0.1	0.073 (0.069)	2.4 ± 0.3
25	HO^-	5.7 ± 0.4	0.25 (0.23)	2.0 ± 0.1	0.090 (0.083)	2.9 ± 0.2
		[6.1 (FA), 5.8 (FA), 6.1 (ICR)]		[2.7 (FA)]		[2.1 (FA), 2.3 (ICR)]
−35	HO^-	6.8 ± 0.5	0.30 (0.27)	3.3 ± 0.1	0.15 (0.13)	2.1 ± 0.2
200	NH_2^-	1.2 ± 0.1	0.054 (0.052)	0.19 ± 0.02	0.0087 (0.0083)	6.3 ± 0.8
160	NH_2^-	1.5 ± 0.1	0.068 (0.064)	. . .	. . .	. . .
100	NH_2^-	2.1 ± 0.2	0.093 (0.087)	0.26 ± 0.01	0.012 (0.011)	8.1 ± 0.8
25	NH_2^-	3.6 ± 0.2	0.16 (0.15)	0.50 ± 0.04	0.022 (0.020)	7.2 ± 0.7
		[4.1 (FA), 4.4 (FA)]		[0.8 (FA)]		[5.5 (FA), 5.6 (ICR)]
−21	NH_2^-	5.0 ± 0.5	0.22 (0.19)	. . .	. . .	. . .
−25	NH_2^-	5.7 ± 0.1	0.24 (0.22)	1.3 ± 0.1	0.056 (0.051)	4.4 ± 0.3

[a] Bimolecular rate constants in units of 10^{-10} cm^3 molecule^{-1} s^{-1}. Error bars represent one standard deviation or 0.1 for rates $\geq 1.0 \times 10^{-10}$ and 0.01 for rates $< 1.0 \times 10^{-10}$, whichever is larger. We estimate that the absolute accuracy for the rate coefficients is ±20%. Literature data are in square brackets and come from [3] and [4] (FA) and 5 (ICR).

[b] Efficiency = k_{obs}/k_{ADO} [37]. Parenthetical values correspond to calculated rates using the method of Su and Chesnavich [38].

[c] Error bars reflect the propagation of the errors in the rate measurements but we estimate that the accuracy is ±20%.

centimeters, and 1.10×10^{-20} is the appropriate conversion factor so that the second-order rate constant (k) is in units of cubic centimeters per particles per s [35]. The reported rate constants were obtained from linear least squares analyses of the slopes of plots of $\ln[A^-]$ versus F_B and are the results of multiple measurements, in some cases over a several year period. Data were collected at ~0.35 Torr over a temperature range from −35 to +200 °C and at 25 °C at pressures of 0.36, 0.61, and 0.81 Torr. In the latter two cases, the pressure of the system was increased by throttling the gate valve to the main pumping system (i.e. the Roots blower). We estimate that the absolute uncertainty in our rate measurements is ±20%.

Product distributions were obtained by two equivalent methods. In the first, the percent change in the reactant ion signal was plotted against the normalized product ion intensities and the data were extrapolated back to time zero (absence of reactant) so as to obtain the initial product distribution. The second method involves normalizing the total ion intensity and plotting the normalized percent change of the reactant ion versus the percent (also normalized) of the observed primary product ions [36]. In this case, straight lines were obtained going through the origin and the slopes of the lines give the branching ratios of the product ions. In either case, the resolution of the resolving quadrupole was decreased until the product ratios were independent of this setting in order to minimize the effects of mass discrimination. Nevertheless, it is unlikely that the absolute uncertainty in the product distributions is better than ±10%.

Commercial samples of diethyl ether (Aldrich Chemical Co.) and diethyl ether-d_{10} (≥99% D, Cambridge Isotope Labs) were stored over lithium aluminum hydride in order to remove small impurities from the vapor above the liquid sample. The ether was also subjected to several freeze–pump–thaw cycles immediately before its use in order to remove any noncondensible impurities.

3. Results and discussion

Both protio and diethyl ether-d_{10} were reacted with amide and hydroxide ions at a variety of temperatures in our variable temperature flowing afterglow device. The relevant rate data, reaction efficiencies (k_{obs}/k_{calc}, where $k_{calc} = k_{ADO}$ or $k_{Su\ and\ Chesnavich}$) [37,38], and kinetic isotope effects (k_H/k_D) at different temperatures are given in Table 1. Each reported rate coefficient corresponds to the average of several experiments each consisting of two or three rate measurements except for the −35 °C diethyl ether-

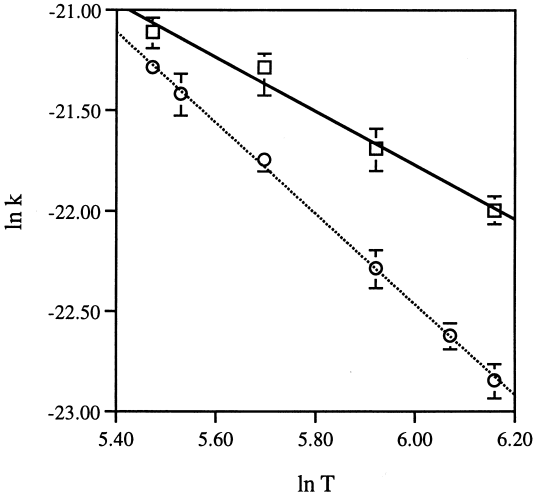

Fig. 1. Temperature dependence of the reaction rates of diethyl ether with hydroxide and amide ions. The squares and the solid line correspond to a linear least squares analysis of the HO^- data [ln $k = -1.34(\ln T) - 13.7$, $r^2 = 0.981$] whereas the circles and the dotted line correspond to the H_2N^- results [ln $k = -2.26(\ln T) - 8.9$, $r^2 = 0.999$].

d_{10} data which are the average of only two determinations with each base. Our room temperature results can be directly compared to those obtained by DePuy and co-workers [3,4] and de Koning and Nibbering [5] in a flowing afterglow and ion cyclotron resonance (ICR) mass spectrometer, respectively. In both cases there is good agreement and the rate data are well within the combined uncertainties of the measurements.

An inverse correlation between rate and temperature is apparent from the data in Table 1. Both the hydroxide and amide ion reactions show rate retardations with increasing temperature. This type of behavior has been observed for a number of gas-phase reactions and has been found to follow the empirical relationship shown in

$$k = cT^n \quad (3)$$

where c is a proportionality constant, T is the temperature in kelvin, and n is the temperature coefficient [39]. The last value gives an indication as to the magnitude of how the rate is affected by temperature. In Fig. 1 we have plotted ln k versus ln T for the hydroxide and amide ion data given in Table 1. A linear correlation is seen in both cases and $n = -1.3$ and -2.3 for HO^- and H_2N^-, respectively. In comparison, other gas-phase reactions have been found to have values ranging from approximately $+1.0$ (proton transfers) to -10.0 (charge transfers). The base-induced elimination of diethyl ether thus displays a modest negative temperature dependence. This result confirms the prediction of a negative temperature dependence by de Koning and Nibbering based upon the qualitative energy dependence of the reaction with hydroxide [5]. It also is in good agreement with the potential energy surface reported by Bierbaum et al. via modeling using statistical rate theory [3]. That is, a negative temperature dependence is found for both the HO^- and NH_2^- reactions, and the latter dependence is larger. The transition states were found to lie 4.6 (HO^-) and 1.6 (NH_2^-) kcal mol^{-1} below the energy of the reactants based upon Rice-Ramsperger-Kassel-Marcus theory, which are in qualitative accord with our activation energies of -0.9 (HO^-) and -1.5 (NH_2^-) kcal mol^{-1} obtained from Arrhenius plots [40]. The relative ordering of the barrier heights is reversed, probably because of the simplicity of the model that was used, but the Arrhenius plots must be curved over the temperature range that was used and the activation energies are qualitative in nature and should not be over interpreted. Our data, nevertheless, are in excellent agreement with the -1.0 kcal mol^{-1} barrier calculated by Gronert using ab initio calculations on a model system ($CH_3CH_2OCH_3 + HO^-$) [9].

It is surprising that diethyl ether reacts faster with hydroxide than amide ion over the temperature range that was examined (from -35 to $+200$ °C) given that the latter base is stronger by 13 kcal mol^{-1} [22]. This result and the similar barrier heights on the potential energy surface can be rationalized if one assumes E1cb-like transition structures for both processes as was done by Bierbaum et al. [3], and which is in accord with Gronert's computations on the hydroxide-induced antiperiplanar elimination of ethyl methyl ether [9]. Binding energies of the initially formed $B^-{\cdot\cdot}Et_2O$ ion complexes are nearly the same when $B^- = HO^-$ and H_2N^- but the cluster energy will be much larger in the corresponding E1cb intermediate

(i.e. $BH\cdot\cdot^{-}CH_2CH_2OCH_2CH_3$) when the base is hydroxide ion; this is based upon MP2/6-31+G(d)//HF/6-31+G(*d*) calculations which were carried out on $B^{-}\cdot\cdot EtF$ and $BH\cdot\cdot^{-}CH_3$, where $B^{-} = HO^{-}$ and NH_2^{-}. Complexation energies for the first species ($B^{-}\cdot\cdot EtF$) are 16.3 (HO^{-}) and 15.0 (H_2N^{-}) kcal mol^{-1}, whereas those for the latter ion complex are 20.9 and 9.5 kcal mol^{-1}, respectively. The better hydrogen bonding ability of water relative to ammonia leads to a stronger interaction, which helps overcome the difference in basicity and is reflected in the activation energies for the transition structures.

Large kinetic isotope effects (KIEs) are observed for the hydroxide and amide ion reactions with diethyl ether as previously noted. Our values, 2.9 ± 0.6 (HO^{-}) and 7.2 ± 1.4 (H_2N^{-}) at 25 °C [41], are somewhat higher than those already noted in the literature [2.1 and 2.3 (HO^{-}) and 5.5 and 5.6 (H_2N^{-})] but are undoubtedly within the combined uncertainties of the measurements [3,5]. When hydroxide is the base, k_H/k_D is largest at 25 °C and falls off monotonically at higher and lower temperatures. The same trend is also observed with amide ion except that the maximum KIE occurs at 100 °C. This behavior is required given the observed temperature dependence of the reaction rate. At low temperatures the reaction efficiency (k_{obs}/k_{calc}) approaches unity and $k_H/k_D \approx 1$, whereas typical Boltzmann behavior at elevated temperatures also leads to an isotope effect of one:

$$k_H/k_D = e^{-\Delta\Delta ZPE/RT} \quad (4)$$

In contrast, de Koning and Nibbering's data indicates that the overall KIE increases with energy in the hydroxide reaction and that the individual isotope effects for the formation of EtO^{-} ($k_H/k_D = 2.20$) and $EtO^{-}\cdot H_2O$ ($k_H/k_D = 1.55$) are unchanged and insensitive to the energy of the system [5]. It is unclear why they observed an increase in the overall isotope effect, but the insensitivity of the individual contributions is not surprising given that the product distribution varies with energy (and temperature, see below). Nevertheless, the isotope effects for the formation of EtO^{-} and $EtO^{-}\cdot H_2O$ must vary with energy. This becomes apparent if one considers the high and low temperature limits. At elevated temperatures the relative proportion of EtO^{-} increases and at some point it probably becomes the only product ion, but the isotope effect approaches 1 so the contribution to the total isotope effect for ethoxide formation must decrease. At reduced temperatures the amount of EtO^{-} decreases until it no longer can form [Eq. (1b), $\Delta H° = +5.5$ kcal mol^{-1}][18], the overall isotope effect goes to 1, and k_H/k_D for the cluster must decrease. Consequently, there is no need to invoke two pathways (syn and anti eliminations) in these reactions as has previously been done. An antiperiplanar elimination followed by a partitioning (with a corresponding isotope effect) between free ethoxide and its solvated product accounts for the experimental results and is in accord with Gronert's ab initio calculations [9]. It also is worth noting that although it was quite reasonable to invoke a syn elimination to account for the solvated product [Eq. (1a)], we have now unequivocally shown in related systems that solvated ions are formed via anti eliminations [11,13].

Initial product distributions for the reactions of diethyl ether with hydroxide and amide ions were measured as a function of temperature. A summary of the results along with literature data at 25 °C are given in Table 2. At room temperature, hydroxide ion has been reported to react with diethyl ether in a flowing afterglow and ion cyclotron resonance mass spectrometer to give ethoxide ion and a water–ethoxide cluster in a 1:2 ratio [4,5]. Amide ion affords the analogous two products under the high pressure conditions in a flowing afterglow, EtO^{-} (85%) and $EtO^{-}\cdot H_3N$ (15%), whereas the solvated ion is not detected under the high vacuum conditions in an ICR. This difference between the FA and ICR results is due to the lack of third-body collisions in an ICR, the greater exothermicity of the amide ion reaction (and hence shorter lifetime of the intermediate complex), and the poorer solvating ability of ammonia.

Our product ratios are in good agreement with the literature flowing afterglow values, but we did note a minor ion (5%) at *m/z* 91 in the HO^{-} reaction. Solvent switching experiments revealed that the identity of this product is hydroxide ion clustered to diethyl ether

Table 2
Product distributions for the reactions of hydroxide and amide ions with diethyl ether at different temperatures[a]

B^-	T (°C)	EtO^- (%)	$EtO^- \cdot BH$ (%)	$Et_2O \cdot B^-$ (%)
HO^-	200	86	14	...
	100	56	44	...
	25	32 [33 (FA), 31 (ICR)]	63 [67 (FA), 69 (ICR)]	5
	−35	22	69	9
NH_2^-	200	100	...	...
	100	99	1	...
	25	91 [85 (FA), 100 (ICR)]	9 [15 (FA), 0 (ICR)]	...
	−35	80	20	...

[a] Literature data are in square brackets and come from [4] (FA) and [5] (ICR).

($HO^-{\cdot}Et_2O$) as opposed to an ethanol solvate of ethoxide ion ($EtO^-{\cdot}EtOH$). For example, it was found that diethyl ether can be washed out with methanol to give $MeO^-{\cdot}H_2O$ (*m/z* 49) and not $EtO^-{\cdot}MeOH$ (*m/z* 77). This product and the others are sensitive to the reaction temperature as shown in Figs. 2 and 3. Solvated ions increase in abundance and ethoxide ion becomes less prevalent as the temperature is lowered whereas the opposite is true when the temperature is increased. This behavior is quite reasonable as clustering is favored at lower temperatures and the formation of EtO^- becomes thermodynamically inaccessible in the reaction with HO^-. At some temperature above 200 °C it appears that EtO^- will become the sole ionic product, presumably because the product ion/molecule complex has a sufficiently short lifetime that the ethoxide ion does not find the ethanol that also is formed. In a similar fashion, the differences in the product distributions in the hydroxide and amide ion-induced eliminations is a reflection of the reaction thermochemistry [Eq. (1)], [18] the poorer solvating ability of ammonia, and the lifetimes of the activated complexes. A more detailed understanding of the product yields would require consideration of the reaction dynamics which is beyond the scope of this work.

The effect of pressure on the reaction rates of diethyl ether with amide and hydroxide ions was examined. Experiments were carried out at room temperature (~300 K) at pressures of 0.36, 0.61, and 0.81 Torr. Under these conditions, the reaction rate is pressure independent with amide ion but increases with pressure with hydroxide ion. The termolecular rate coefficient ($k_{III} = 2.6 \times 10^{-26}$ cm^6 $molecules^{-2}$ s^{-1}) was determined in the latter case from the slope of the line of a plot of the second-order rate versus pressure (Fig. 4). This is the rate associated with the stabilization of the activated complex ($HO^-{\cdot}Et_2O$)* through collisions with helium atoms. The observed pressure dependence is consistent with a bimolecular reaction which has a negative temperature dependence since collisions between the buffer gas and ($HO^-{\cdot}Et_2O$)* will dissipate some of the excitation energy and facilitate product formation [39,42]. In

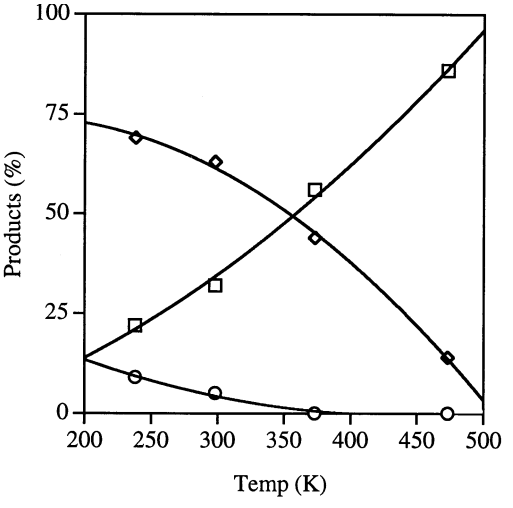

Fig. 2. Product ratios from the reaction of diethyl ether with hydroxide ion as a function of temperature. Squares represent EtO^-, diamonds are for $EtO^-{\cdot}H_2O$, and circles depict $Et_2O{\cdot}\ HO^-$. The solid lines are simply for visualization purposes.

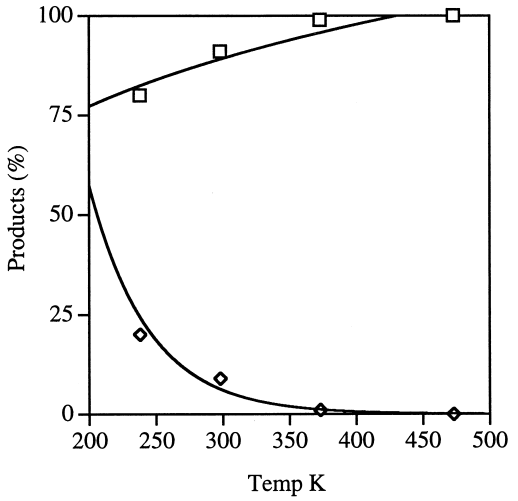

Fig. 3. Product ratios from the reaction of diethyl ether with amide ion as a function of temperature. Squares represent EtO^- and diamonds are for $EtO^-{\cdot}H_3N$. The solid lines are simply for visualization purposes.

contrast, the activated complex in the amide ion reaction presumably has a shorter lifetime so the relatively small changes in pressure do not effect the rate at 25 °C.

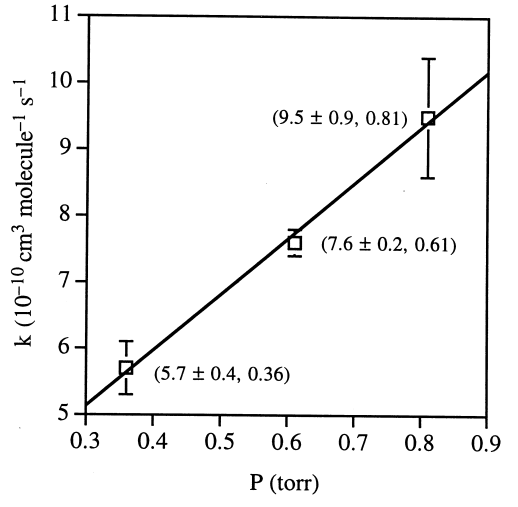

Fig. 4. Bimolecular rate coefficients vs. pressure for the reaction of diethyl ether with hydroxide ion. Parenthetical values correspond to the reaction rate at the given pressure, and the solid line represents a linear least squares fit of the data [$k = (8.41)P + 2.61$, $r^2 = 0.996$].

4. Conclusions

A modest negative temperature dependence was found for the hydroxide and amide ion-induced elimination reactions of diethyl ether. Barrier heights from -1 to -2 kcal mol^{-1} relative to the separated reactants were found and are in accord with previous predictions based upon statistical rate theory and ab initio calculations. Large kinetic isotope effects were measured and found to monotonically decrease from the maximum value by raising or lowering the temperature. Increasing the magnitude of a primary kinetic isotope effect by varying the temperature, consequently, will be of limited value. In general, only those transformations with positive activation energies will be particularly sensitive to temperature, and in these cases the overall rate will decrease as the temperature is lowered to increase the isotope effect.

The product distributions are sensitive to the reaction temperature. Ethoxide ion dominates at elevated temperatures whereas solvated product ions are much more abundant at lower temperatures. A new product ion, $HO^-{\cdot}Et_2O$, also was seen. These results are in accord with a reaction which proceeds *via* an anti elimination followed by a distribution of the products into free and solvated ions.

Finally, the effect of pressure on the reaction rates was studied. The amide ion-induced elimination is independent of pressure from 0.3 to 1 Torr, whereas the hydroxide reaction rate increases by 70% in going from 0.36 to 0.81 Torr.

Acknowledgements

The authors wish to thank Professor Maurice Kreevoy for helpful discussions. Support from the National Science Foundation, the donors of the Petroleum Research Foundation, as administered by the American Chemical Society, the Minnesota Supercomputer Institute and the University of Minnesota–IBM Shared Research Project are gratefully acknowledged.

References

[1] C.K. Ingold, Structure and Mechanism in Organic Chemistry, 2nd ed., Wiley, Ithaca, 1969.
[2] W.H. Saunders Jr., A.F. Cockerill, Mechanisms of Elimination Reactions, Wiley, New York, 1973.
[3] V.M. Bierbaum, J. Filley, C.H. DePuy, M.F. Jarrold, M.T. Bowers, J. Am. Chem. Soc. 107 (1985) 2818.
[4] C.H. DePuy, V.M. Bierbaum, J. Am. Chem. Soc. 103 (1981) 5034.
[5] L.J. de Koning, N.M.M. Nibbering, J. Am. Chem. Soc. 109 (1987) 1715.
[6] C.H. DePuy, E.C. Beedle, V.M. Bierbaum, J. Am. Chem. Soc. 104 (1982) 6483.
[7] C.H. DePuy, S. Gronert, A. Mullin, V.M. Bierbaum, J. Am. Chem. Soc. 112 (1990) 8650.
[8] S. Gronert, C.H. DePuy, V.M. Bierbaum, J. Am. Chem. Soc. 113 (1991) 4009.
[9] S. Gronert, J. Am. Chem. Soc. 114 (1992) 2349.
[10] J.J. Rabasco, S.R. Kass, Tetrahedron Lett. 32 (1991) 4077.
[11] J.J. Rabasco, S.R. Kass, J. Org. Chem. 58 (1993) 2633.
[12] J.J. Rabasco, S.R. Kass, Tetrahedron Lett. 34 (1993) 765.
[13] J.J. Rabasco, S. Gronert, S.R. Kass, J. Am. Chem. Soc. 116 (1994) 3133.
[14] K. Seemeyer, T. Prusse, H. Schwarz, Helv. Chim. Acta 76 (1993) 113.
[15] W.W. van Berkel, L.J. de Koning, N.M.M. Nibbering, J. Am. Chem. Soc. 109 (1987) 7602.
[16] F.M. Bickelhaupt, G.J.H. Buisman, L.J. de Koning, N.M.M. Nibbering, E.J. Baerends, J. Am. Chem. Soc. 117 (1995) 9889.
[17] M.E. Jones, G.B. Ellison, J. Am. Chem. Soc. 111 (1989) 1645.
[18] All thermochemistry comes from [19–22].
[19] J.D. Cox, G. Pilcher, Thermochemistry of Organic and Organometallic Compounds, Academic, New York, 1970.
[20] J.E. Bartmess, Secondary Negative Ion Energetics Data, November 1998, National Institute of Standards and Technology, Gaithersburg, MD, 20899 (http://webbook.nist.gov).
[21] H.Y. Afeefy, J.F. Liebman, S.E. Stein, Secondary Neutral Thermochemical Data, November 1998, National Institute of Standards and Technology, Gaithersburg, MD 20899 (http://webbook.nist.gov).
[22] S.G. Lias, J.E. Bartmess, J.F. Liebmann, J.L. Holmes, R.D. Levin, W.G. Mallard, J. Phys. Chem. Ref. Data 17 (1988) 647–796 (Suppl 1) [or the slightly updated form available on a personal computer, NIST Negative Ion Energetics Database (Version 3.00, 1993); NIST Standard Reference Database 19B].
[23] It has been shown that the solvated alkoxide does not arise from clustering of the free ethoxide. See [4] for further details.
[24] S. Gronert, J. Am. Chem. Soc. 113 (1991) 6041.
[25] S. Gronert, J. Am. Chem. Soc. 115 (1993) 652.
[26] S. Gronert, G.N. Merrill, S.R. Kass, J. Org. Chem. 60 (1995) 488.
[27] S. Gronert, S.R. Kass, J. Org. Chem. 62 (1997) 7991.
[28] G.N. Merrill, S. Gronert, S.R. Kass, J. Phys. Chem. A 101 (1997) 208.
[29] T. Minato, S. Yamabe, J. Am. Chem. Soc. 107 (1985) 4621.
[30] T. Minato, S. Yamabe, J. Am. Chem. Soc. 110 (1988) 4586.
[31] F.M. Bickelhaupt, E.J. Baerends, N.M.M. Nibbering, T. Ziegler, J. Am. Chem. Soc. 115 (1993) 9160.
[32] F.M. Bickelhaupt, E.J. Baerends, Chem. Eur. J. 2 (1996) 196.
[33] M.R. Ahmad, S.R. Kass, J. Am. Chem. Soc. 118 (1996) 1398.
[34] S.R. Kass, H. Guo, G.D. Dahlke, J. Am. Soc. Mass Spectrom 1 (1990) 366.
[35] In all cases, we assume that the average ion velocity is 1.60 times the average helium velocity as has typically been done. See (a) E.E. Ferguson, F.C. Fehsenfeld, A.L. Schmeltekopf, in Advances in Atomic and Molecular Physics, D.R. Bates and I. Estermann (Eds.), Academic, New York, 1969, Vol. 5, pp. 1–56; (b) B.L. Upschulte, R.J. Shul, R. Passarella, R.G. Keese, A.W. Castleman, Int. J. Mass Spectrom. Ion Processes 75 (1987) 27 for further details.
[36] J.J. Grabowski, L. Zhang, J. Am. Chem. Soc. 111 (1989) 1193.
[37] T. Su, M.T. Bowers, Int. J. Mass Spectrom. Ion Phys. 12 (1973) 347.
[38] T. Su, W.J. Chesnavich, J. Chem. Phys. 76 (1982) 5183.
[39] M. Meot-ner, Temperature and pressure effects in the kinetics of ion-molecule reactions, in Gas Phase Ion Chemistry, M.T. Bowers (Ed.), Academic, New York, 1979, Vol. 1, pp. 197–271.
[40] Least-squares analyses of the Arrhenius plots gives the following equations: $y = (0.43)x - 22.9$, $r^2 = 0.954$ (HO^-) and $y = (0.74)x - 24.3$, $r^2 = 0.988$ (H_2N^-). Omission of the lowest temperature points, where the curvature will be greatest, leads to better correlations but only small changes (0.2 kcal mol^{-1}) in the activation energy.
[41] The cited errors correspond to our estimate of the uncertainty, ±20%, as this is larger than the propagation of the uncertainties in the individual rate constants.
[42] M.E. Crestoni, S. Fornarini, M. Lentini, M. Speranza, J. Chem. Soc. Chem. Commun. 1995 (1995) 121.